IOSR Journal of Applied Physics (IOSR-JAP)
e-ISSN: 2278-4861.Volume 7, Issue 2 Ver. III (Mar. - Apr. 2015), PP 17-26
www.iosrjournals.org

Impedance, Electrical Conductivity and Piezoelectric Studies on Nb^{5+} doped $(Bi_{0.5}Na_{0.5})_{0.94}Ba_{0.06}TiO_3$ -PVDF 0-3 composites

Amrita Singh[1], Kumar Amarnath[2,] Kamal Prasad[1,2], and Ashutosh Prasad[1*]
[1]*University Department of Physics, T.M. Bhagalpur University, Bhagalpur 812007 India*
[2]*Aryabhatta Centre for Nanoscience and Nanotechnology, Aryabhatta Knowledge University, Patna 800001 India*

Abstract: *The present work makes use of experimental ac complex impedance data to obtain the electrical parameters like electrical conductivity and activation energy of ($(Bi_{0.5}Na_{0.5})_{0.94}Ba_{0.06}TiO_3$+0.2 wt%$Nb_2O_5$)–PVDF 0-3 composites with 10, 20 and 30 vol. percentage of ($(Bi_{0.5}Na_{0.5})_{0.94}Ba_{0.06}TiO_3$+0.2 wt%$Nb_2O_5$) in the frequency range 1kHz–1 MHz over a temperature range of 35°C-145°C. SEM micrographs exhibited good dispersion of almost spherical dense grains (sizes ranging between 8-14 μm). Cole-Cole analysis for frequency-dependent complex impedance data indicated the presence of grain-boundary effect along with the bulk contribution, thereby showing the NTCR character for the composites, especially in the lower frequency and higher temperature regime. Results were also analyzed via the electric modulus formalism. Experimental results evidenced that the recorded relaxation phenomena include contributions from both the polymeric matrix and the presence of the reinforcing phase. Temperature dependent ac conductivity data also endorsed the NTCR character for the composites. Activation energy data allowed an insight into the mechanism of hopping of charge carriers in the materials. Ceramic filler concentration dependent increase of d_{33} (ranging between 20-40 pC/N) of the composite was seen to follow the first order exponential growth type of equation.*

Keywords: *Ceramic-polymer 0-3 composites; Grains /grain-boundaries; piezoelectric ceramics; Complex impedance/modulus spectroscopy; AC conductivity*

e-mail id of the corresponding author: apd.phy@gmail.com

I. Introduction

During the last few years, increased global environmental concern has prompted considerable efforts to reduce the quantity of hazardous substances, like the highly toxic lead, in electronic consumer products. Regulatory agencies on global level have begun putting strict restrictions on the use of lead, however with the exception of the electronics and electromechanical devices industry, in view of the lack of a suitably harnessed lead-free material having comparable properties with those of (Pb, Zr)TiO_3 (PZT), containing toxic lead.

Piezoelectric ceramics have, in general, large dielectric constant, high piezoelectric charge coefficient as well as acoustic impedance, whereas polymers have generally lower dielectric constant and acoustic impedance close to that of water as well as of human body tissue. This low value of acoustic impedance combined with higher values of piezoelectric voltage coefficients for piezoelectric polymers makes the piezoelectric ceramic-polymer composites suitable candidates for dielectric, ferroelectric, piezoelectric, pyroelectric, electro-optic, as well as superconducting properties in micro-devices making good strain-monitoring and hydrostatic sonar sensors [1]. Moreover, these ceramic-polymer composite materials have been suggested to be viable alternative tools in piezoelectric and pyroelectric transducer as well as in energy harvesting applications [2-6]. Hence, piezoelectric composites are now treated as established alternatives to conventional ferroelectric ceramic materials as well as to the more recently discovered ferroelectric polymers. In short, these systems form the basis of current area of active research activities and have received intensive global attention [7-10] in view of the fact that these composites, having excellent dielectric and mechanical properties, can be prepared under lower temperature conditions and can be designed according to specific requirements by tailoring the relative fraction of the filler materials. Recently, there has been a great interest in a new generation of composite materials exhibiting superior dielectric properties with lower cost, size, weight, and easy processibility [11–15]. Composite systems, which are apt for variation of some of their properties (such as shape, natural vibration frequency, damping coefficient, polarization etc) in a controllable fashion under the influence of an external stimulus, are considered as adaptive or smart materials [16–18].

In an attempt to provide lead-free perovskite ceramic materials having optimal dielectric and piezoelectric properties, Takenaka [19], Wang et al [20], Wu et al [21], Li et al [22] as well as the present group of workers [23] worked with some of the lead-free materials and reported that $(Na_{1/2}Bi_{1/2})_{0.94}Ba_{0.06}TiO_3$, the morphotropic phase boundary (MPB) composition, is one of the most suited lead-free materials for its use in electronic and electromechanical devices. However, from these studies it transpired that although BNBT-*x* ceramics are seen to possess good piezoelectric properties near the MPB, the gap still exists in between the

comparable ferroelectric and electromechanical properties of these ceramics with those of PZT. In order to further improve the properties of BNBT-*x* ceramics, some additions, including Nb^{5+} at the B- sites of ABO_3 type of perovskite structures, have been suggested for specific applications [24-28]. Some of these studies reveal that the doping of Nb^{5+} enhanced the piezoelectric coefficient, however at the cost of increased dielectric loss tangent (tan δ), of BNBT-*x* ceramics. On the basis of a systematic study on the samples having different Nb^{5+} doping levels (0.2-1.0 wt%), the present group of workers observed that the $(Na_{1/2}Bi_{1/2})_{0.94}Ba_{0.06}TiO_3$(BNBT6), the morphotropic phase boundary (MPB) composition doped with 0.2 wt% Nb^{5+} exhibited optimal dielectric, and piezoelectric properties.

As far as the polymer phase of the biphasic composite(s) is concerned, piezoelectric polymer PVDF, despite many of its deficient properties, has appeared appealing to numerous industries for its inexpensive, lightweight, biologically compatible and mechanically stable structures. It can undertake large amount of deformation while sustaining large forces. It has expeditious response time, very low density, and notable flexibility when compared to those of electro-active ceramics and shape memory alloys. The piezoelectric PVDF and its copolymers are widely applied materials in both actuation and sensing mechanisms. They can be utilized as fibers and films as energy harvesters in linear movement requirements in various engineering applications such as active micro air vehicle wings, piezo -laminated columns, and shape correction films in space applications, endoscopic tactile sensors and macro-fluidic control [12, 13, 27].

Literature survey on the above referred topic revealed that the complex impedance/modulus, ac conductivity and piezoelectric studies on $((Bi_{0.5}Na_{0.5})_{0.94}Ba_{0.06}TiO_3$+0.2 wt% $Nb_2O_5)$–PVDF ((BNBT6N0.2)-PVDF) 0-3 composites with different contents of BNBT6N0.2 have not been undertaken in the recent past. In view of the above, the present work relating to the study of the electrical properties of ((BNBT6N0.2)-PVDF) 0-3 composite samples having 10, 20 and 30 volume percent of BNBT6N0.2 powder was undertaken via complex impedance/electric modulus spectroscopic, electrical conductivity and piezoelectric properties' analyses.

II. Materials and Methods

Polycrystalline samples of ceramic solid solutions of (BNBT6) were prepared by the conventional high-temperature solid-state reaction technique at 1170ºC for about 3h. The XRD patterns were observed on BNBT6N0.2 powder at the ambient temperature with an X-ray diffractometer (X'pert-PRO, USA), using CuK_α radiation (λ=1.5405 Å) over a broad range of Bragg angles ($20^o \leq 2\theta \leq 80^o$). The obtained XRD pattern did not fit to any single space group model (including monoclinic Cm, tetragonal P4mm, or rhombohedral R3c), whereas it could be fitted to the Cm+P4mm mixed phases. This observed co-existence of two phases confirmed a tetragonal side of the monoclinic/tetragonal MPB composition. Hence, these patterns for the ceramic were fitted with the tetragonal unit cell structure. The calcined powder was again ground using an agate mortar and pestle and then 0.2 wt. % Nb_2O_5 was added to it and mixed thoroughly in dry as well as in wet acetone medium. A part of the dried powder was then pressed into discs using pressure of 200MPa in a hydraulic press with 5 wt% PVA solution added as a binder. The fabricated compact green pellets were sintered at an optimized temperature of 1175º for about 2h. The frequency and temperature dependent dielectric constant (ε_r) and loss tangent (tan δ), complex impedance (Z^*) and phase angle (θ) of the sintered ceramic samples were measured using a computer-controlled LCR Hi-Tester (HIOKI 3532-50, Japan) on a symmetrical cell consisting of Ag │ ceramic │ Ag, where Ag is a conductive paint coated on each side of the pellet. The ceramic sample was poled under an applied DC electric field of 2.5kV/mm at 80°C in a silicone oil bath. Longitudinal piezoelectric charge coefficients (d_{33}) of the poled ceramic samples were measured at the room temperature using a PM3500 d_{33} / d_{31} meter (KCF Technologies, USA). Now, ((BNBT6N0.2)-PVDF) 0-3 composite samples having 10, 20 and 30 volume percentage of calcined BNBT6N0.2 powder were prepared by solution cast method (using DMF as the solvent for PVDF) at an elevated temperature (~70°C-80°C) under constant stirring with the help of a magnetic stirrer and ultrasonic agitator. The composite samples in the molten (viscous) state were poured into cylindrical and rectangular stainless steel dies and were then allowed to dry for a few days in open air. The fabricated composites were taken out of the dies and were then cut into the disk-shaped pieces of suitable thicknesses. They were allowed to dry for a few days further before any measurements on them were made. The green samples were then polished and painted on both sides by the use of high grade silver paste. Microstructures of the fabricated composites were observed at the ambient temperature by using a scanning electron microscope (JEOL-JSM840A).The complex impedance (Z^*) and phase angle (θ) of the different composite samples were measured in the frequency range 1kHz-1MHz between the ambient temperature and 145°C by the same computer interfaced LCR Hi-Tester (HIOKI 3532-50, Japan) in the same way as for the ceramic samples. Longitudinal piezoelectric charge coefficients (d_{33}) of the poled composite samples were measured at the ambient temperature using a PM3500 d_{33} / d_{31} meter (KCF Technologies, USA). The poling of the composite samples was done under an applied DC electric field of about 1.5kV/mm at 80 °C in a silicone oil bath for about 15 minutes because the composite samples were seen to be unable to withstand higher field strengths than 1.5kV/mm and higher dwell time on account of leakage currents,

III. Results and discussion

3.1 Microstructural analysis

Fig. 1(a), (b), and (c) shows the EDAX patterns and SEM micrographs (insets) for the ((BNBT6N0.2)-PVDF) 0-3 composites having (a) 10, (b) 20 and (c) 30 vol. % of BNBTN0.2 ceramic fillers. SEM micrographs showed homogeneous distribution of dense grains for all the compositions and the EDAX patterns confirmed the presence of different constituent elements of the composite like Bi, Na, Ba, Ti, O, C, Nb *etc*. SEM micrographs (shown separately in Fig. 2(a), 2(b), and 2(c)) revealed that the grains are spherical in shape for all the fabricated composite samples having their sizes ~8.5 μm, 12.5μm, and 14μm, respectively, for 10, 20 and 30 volume percentage of BNBT6N0.2 powder.

3.2 Complex impedance analysis

Most of the real ceramics contain grains and grain-boundary regions, which individually have very different physical properties and are well observed in the impedance and modulus spectra. Electrical *ac* data may be presented in any of the four interrelated formalisms: Relative permittivity ($\varepsilon^* = \varepsilon' - j\varepsilon''$ (the real part being given by C/C_0 where $C \sim C_{parellel}$ is directly given by the LCR Hi-Tester); Impedance ($Z^* = Z' + jZ'' = 1/j\omega C_0\varepsilon^*$, where Z' ($=|Z^*|\cos\theta$) *is* the real part of complex impedance ; $|Z^*|$ and θ are directly given by the computer-controlled LCR Hi-Tester; Electric modulus ($M^* = M' + jM'' = 1/\varepsilon^*$; Admittance ($Y^* = Y' + jY'' = j\omega C_0\varepsilon^*$; and $\tan\delta = \varepsilon''/\varepsilon' = M'/M'' = Z''/Z' = Y'/Y''$, where $\omega(=2\pi f)$ is the angular frequency; C_0 ($= \varepsilon_0 A/t$) is the geometrical capacitance; $j = \sqrt{-1}$; ε_0 is the permittivity of free space ($=8.854\times10^{-12}$ Fm^{-1}); t is the thickness and A the area of the pellet; δ is complementary to the phase angle (θ). However, the present work is confined to the use of only the impedance/modulus data for the entire analysis.

Fig. 3 (a)-(f) shows the $Z'(f)$ and $Z''(f)$ plots for ((BNBT6N0.2)-PVDF) 0-3 composites having (i) 10, (ii) 20 and (iii) 30 vol. % of BNBT6N0.2 ceramic fillers at several temperatures between ambient temperature and 145°C. The plots reveal that at lower temperatures, Z' values decrease monotonically with increasing frequency up to a certain limiting value (~10 kHz) above which Z' becomes almost frequency- independent. The higher values of Z′ at lower frequencies and higher temperatures indicate that the polarization in the test material is comparatively larger at these frequencies and temperatures. The temperature where this frequency-dependent to frequency-independent change of Z' occurs, varies with frequency in different material compositions. This also signifies that the resistive grain boundaries become conducting at these temperatures and that the grain boundaries are not relaxing even at the highest measurement ranges of frequency and temperature. $Z''(f)$ plots showed almost identical monotonically decreasing type of variation up to a certain frequency limit ~10kHz beyond which they are seen to merge together at a very low value of Z'' to show frequency- independent nature of variation extending up to the highest frequency limit at all the chosen temperatures. The merger of Z″ (as well as of Z′) at higher frequencies for all the temperatures indicate possible release of space charge polarization/accumulation at the boundaries of homogeneous phases in the test material system under the applied external field. At lower temperatures, monotonic decrease of Z″ indicated that at lower temperatures the relaxation is almost absent in the material system. This means that relaxation species are immobile defects to which only the orientation effects may be associated. Also, the decreasing magnitudes of Z′ and Z″ with increasing frequencies imply that relaxation in the material system is temperature-dependent, and there is apparently not a single relaxation time. Fig. 3 (g) - (h) shows the frequency dependent variation of real and imaginary parts (Z' and Z''), respectively, for the three compositions at the room temperature. From the plots it is seen that at the lowest range of measurement frequency (~1 kHz) the magnitude of Z' decreases from ~2.89 MΩ to 2.51 MΩ with increase in volume content of the ceramic filler from 10% to 30%. However, the trend of ceramic filler concentration dependent variation of Z'' in the lower frequency region is just opposite to that of Z' in the sense that it increases from ~10.79 MΩ to 11.21 MΩ with an increase in volume content of the ceramic filler from 10% to 30%, thereby indicating an increased resistive grain boundaries' contribution with increase in volume content of the ceramic filler in the composite.

The electrical properties of the present composite material system have been first investigated using Complex Impedance Spectroscopy (CIS) technique. The Nyquist plots between Z′ (f) and $Z''(f)$ (for the sake of convenience, only the modulus of Z'' has been used in all of the plots drawn in the present work, whereas actually it is - Z'') for (BNBT6N0.2)-PVDF 0-3 composites having (a) 10, (b) 20 and (c) 30 vol. percentage of NBT6N0.2 at different temperatures between 35-145°C have been shown in Fig. 4(a)-(c). The impedance spectrum is distinguished by semicircles. A series array of lone parallel RC combination (R_g, C_g) in series with a resistor (R_s) (though the almost frequency-independent data of R_s are not shown in any of the plots, for brevity sake) was found to best fit the experimental data for the given composition, thereby indicating the dominance of bulk contributions from intrinsic grains in the samples. No other relaxation mechanism, such as the grain-boundaries or electrode effects in the sample could be identified through the CIS technique in the studied frequency range. The resulting curves for the composite having 30 volume percentage of the ceramic filler, as shown in Fig.4(c), showed a comparatively better tendency to bend towards the abscissa to form semicircles

with their centers below the real axis, having comparatively larger radii and the radii decreasing with the increase of temperature, thereby representing the distribution of relaxation times in the test sample and indicating a decrease in the resistivity of the material with a clear-cut departure from the ideal Debye type behaviour. With increasing temperature, intercept points on the real axis are shown to shift towards the origin, thereby showing the NTCR character of the test composite samples.

3.3 Complex modulus analysis

Complex modulus analysis is an alternative approach to explore electrical properties of the material and magnify any other effects present in the sample (which are unidentifiable or superimposed in CIS technique) as a result of different relaxation time constants. Electric modulus is defined as the inverse of complex permittivity by the Equation (1) given below:

$$\varepsilon^*(\omega)\times M^*(\omega)=1\Rightarrow$$
$$M'(\omega)=M'(\omega)+jM''(\omega)=1/\varepsilon^*(\omega)=\left[\varepsilon'(\omega)/(\varepsilon'(\omega)^2+\varepsilon''(\omega)^2)+\varepsilon''(\omega)/(\varepsilon'(\omega)^2+\varepsilon''(\omega)^2)\right] \quad (1)$$
$$=j\omega C_0 Z^*(\omega)=j\omega C_0(Z'(\omega)-jZ''(\omega))$$

Fig. 5(a) and 5(b) shows the complex modulus plane Nyquist plots for these compositions (having 10, 20, and 30 vol. percentages of BNBT6N0.2 corresponding to the two higher measurement temperatures i.e., at 90^{o}C and 100^{o}C. Both the plots corresponding to the two temperatures are seen to be almost identical in shape and size. These semicircles indicate that both grain and grain boundary capacitance started playing their active roles in the conduction mechanism of the material system at higher temperatures. The intensities of the peaks are seen to diminish with increase of the content of BNBT6N0.2 ceramic particles and at the same time they are seen to slightly shift towards lower frequency side at the higher concentrations. From the definition and formulation of electric modulus given in Equation (1), decreasing values of (M'') correspond to enhanced values of dielectric loss index (ε'') and thus, to a more pronounced relaxation phenomenon. Increased values of dielectric loss signify that the relative effect consumes more energy. These results indicate that the kinetics of α-relaxation process, which is associated with glass- to- rubber transition in ceramic-polymer composites and is a characteristic phenomenon dominant at low frequencies~0.1Hz (that is outside our experimental frequency range/window), is modified or lessened by the amount of ceramic particles and, in particular, the whole process becomes slower as the amount of ceramic filler increases.

3.4 Electrical conductivity analysis

The real part of ac conductivity is given by following equation:

$$\sigma_{ac}=\omega\varepsilon_o\varepsilon'' \quad (2)$$

Thus, σ_{ac} is directly related to the dielectric properties of the material. Alternatively, the real part of the dominant bulk conductivity may be evaluated from the impedance spectrum using the relation $\sigma_{ac} = t / (Z'A)$; where Z' (=|Z*|cosθ) *is* the real part of complex impedance. As referred to earlier, the second formulation has been used in the present study.

Fig. 6 shows the log-log plot of the real part of ac electrical conductivity (σ_{ac}) versus frequency at different temperatures for ((BNBT6N0.2)-PVDF) 0-3 composites having 30 vol. percentage of BNBT6N0.2 filler. The plots reveal that the real part of ac conductivity of the present composite material does not change appreciably in the measurement ranges of frequency (from 1 kHz to 1MHz) and temperature (from the temperature of ambience to 145^{o}C). Further, all the $\sigma_{ac}(f)$ curves were found to be merging at high frequencies (at ~500kHz) above which an opposite dispersion was observed, thereby suggesting the less defect mobility and low conductivity in the material system [29]. However, each of the curves indicated at least two slopes-one in the lower and the other in the higher frequency region, as clearly depicted in Fig. 6. The frequency and temperature dependence of ac conductivity data for the ((BNBT6N0.2)-PVDF) 0-3 composites correspond to the hopping type of conduction. Applying JRM to the frequency response, experimental conductivity data for the ((BNBT6N0.2)-PVDF) 0-3 composites were found to fit the Jonscher's modified double power law [30-36] given as:

$$\sigma_{ac}=\sigma_o+A\omega^{S_1}+B\omega^{S_2} \quad (3),$$

where σ_o is the frequency independent (electronic or dc) part of ac conductivity. The exponent s_1 ($0 \leq s_1 \leq 1$) corresponds to the low frequency region *i.e.*, to the grain-boundary conductivity, pertaining to translational ion hopping whereas the exponent s_2 ($0 < s_2 < 2$) characterizes the high frequency region i.e., to the grain conductivity indicating the existence of well localized relaxation/re-orientational process [30], the activation energy of which is ascribed to the reorientation ionic hopping. In the jump relaxation model (JRM) introduced by Funke [31] and extended by Elliot [32] to account for ionic conduction in solids, there is a high

probability for a jumping ion to jump back (unsuccessful hop). However, if the neighborhood becomes relaxed with respect to the ion's position, the ion stays in the new site. The conductivity in the low frequency region is associated with successful hops. Beyond the low frequency region, many hops are unsuccessful and as the frequency increases, there is higher possibility of more hops to be unsuccessful. The change in the ratio of successful to unsuccessful hops is seen to result in dispersive conductivity in the test material(s). In the perovskite type oxide materials, presence of charge traps in the band gap is expected. The JRM suggests that different activation energies are associated with unsuccessful and successful hopping processes.

Fig. 7(a)-(c) shows the $\ln(\sigma_{ac})$ *vs.* $1000/T$ plots for the three compositions i.e., (BNBT6N0.2)-PVDF 0-3 composites with 10, 20, and 30 vol. percentage of BNBT6N0.2 filler at different indicated frequencies (1kHz, 10kHz, 100kHz, and 1MHz). In the low temperature regime, ac conductivity of all the compositions was seen to increase sharply with increase in frequency, thereby indicating dispersion of conductivity with frequency. With increase in temperature, dispersion in conductivity narrowed down and all the curves for different frequencies showed a tendency to merge at high temperatures, although they didn't merge completely in the chosen range of temperature. The conductivity of the materials was found to increase with increase in temperature, and merger of the conductivity curves in the higher temperature region is assumed to result with the release of space charge. The enhancement in conductivity with temperature may be considered on the basis that within the bulk, the oxygen vacancies due to the loss of oxygen (usually created during sintering) allow the charge compensation process following the Kröger-Vink equation [33]: $O_o \rightarrow \frac{1}{2}O_2 \uparrow +V_o^{\bullet\bullet} + 2e^{-1}$ to occur, thereby showing that free electrons are left behind in the process, making the materials n-type. The activation energy for conduction was obtained using the Arrhenius relationship:

$$\sigma_{ac} = \sigma_o \exp(-E_a / k_B T) \qquad 4(a)$$

$$\text{whence } \ln(\sigma_{ac}) = \ln(\sigma_o) - E_a / k_B T \qquad 4(b)$$

The slope of the linear least- squares- fit of the ac conductivity data to Eq. 4(b) gives the value of the apparent activation energy, E_a. Using Arrhenius relation (Eq. 4), the ac activation energies were calculated in the higher temperature region at 1kHz and 10 kHz and the values for the composite having 30 vol. % of the ceramic filler are given in the Table 1. It is observed that ac conductivity-based activation energies computed at higher frequencies are lower than those at lower ones in the same temperature range. The ac conductivity-based activation energy values are found to increase sharply with increase in temperature. The activation energies for ((BNBT6N0.2)-PVDF) 0-3 composites having 30 volume percentage of BNBT6N0.2 were found to be ~0.135-0.596eV at 1 kHz and ~0.080-0.644eV at 10 kHz in the higher temperature region (115-145^{o}C), thereby suggesting that the conductivity may be the result of defects and associated charge carriers of metal ions such as Na^{+}, Bi^{3+}, and Ba^{2+} at the A-site and Ti^{4+}, Ti^{3+} and Nb^{5+} at the B-site in the ceramic phase of the composite. At higher sintering temperatures, bismuth ions are the first to get evaporated and thereby oxygen vacancies are created for charge neutralization. Defects such as bismuth $V_{Bi}^{\bullet\bullet\bullet}$ and oxygen vacancies $V_O^{\bullet\bullet}$ are considered to be the most mobile charges and play an important role in polarization fatigue and conduction [32]. However, the conductivity based activation energies for the other two compositions (having. 10 and 20 volume % of the ceramic filler) were found to be unreliable for analysis in the sense that these composites exhibited very high order of magnitude for resistivity, as indicated in Fig. 3 as well as in Fig. 4 and at this high order of magnitude for resistivity, the complex impedance Nyquist plots have been treated to be unreliable.

3.5 Piezoelectric characterization

Measured value of longitudinal piezoelectric charge coefficient (d_{33}) of host polymer (PVDF) was found to be equal to 4 pC/N [18] while that of the ceramic filler $(Bi_{0.5}Na_{0.5})_{0.94}Ba_{0.06}TiO_3$ doped with 0.2wt% of Nb_2O_5 (BNBT6N0.2) it was found to be equal to 150pC/N. The d_{33} values for the composites having 10, 20, and 30 volume percent of BNBT6N0.2 were found to be ~20, 25, and 40 pC/N, respectively.

The ceramic filler concentration dependence of experimentally measured effective d_{33} of 0.2 wt% Nb_2O_5 doped $(Bi_{0.5}Na_{0.5})_{0.94}Ba_{0.06}TiO_3$ -PVDF 0-3 composites are shown in Fig. 8. In an attempt to provide an acceptable model for the ceramic (filler) concentration dependent variation of piezoelectric constant (d_{33}) of the test composite materials under the present study, the first order exponential growth type of mathematical model in the form $Y = Y_o + A \exp(x/\tau)$ (where Y_o, A and t or β (= $1/\tau$) are the model parameters and x is the volume fraction of ceramic in the composite) was found suitable. The value of r^2 is ~0.99658, thereby showing good agreement between theoretical and experimental results. In the present context, the term $(Y_o + A)$ corresponds to the d_{33} value at $x = 0$ *i.e.* for the polymer matrix, while the term $[Y_o + A \exp(\beta)]$ for $x = 1$ corresponds to the value for the ceramic filler. Here β $(=1/\tau) \approx 0.6459$ may be designated as the filler concentration dependent "piezoelectric coefficient growth parameter". From the study it transpired that if quite different types of ceramic fillers as well as polymer matrices were chosen as the test materials, the filler concentration dependent growth parameter (β) for piezoelectric constant would certainly assume different values, at least due to the different nature of densification of the samples (lighter polymer particles being replaced by denser ceramic particles), as

the ceramic concentration is increased. The growth may also be ascribed to the different ratios of ac conductivity values for ceramic to those for polymer phases (which are generally greater than 1) in the composite. Thus, it is expected that the values of β for different test composite materials might throw some light on the nature of such type of variation (sharp or flat) and could thus assume a type of calibration parameter, which may be useful for further studies. The effective piezoelectric coefficient of the composite as a function of ceramic content can be expressed in the form:

$$(d_{33})_{eff} = -153.38864 + 159.00789 \exp(0.6459x) \quad (r^2=0.99658) \qquad (5)$$

where x ($0 \leq x \leq 1$) is the volume fraction of the ceramic filler (0.2% Nb_2O_5 doped $(Bi_{0.5}Na_{0.5})_{0.94}Ba_{0.06}TiO_3$) in the composite.

IV. Conclusions

The present work describes the impedance, electric modulus and conductivity studies on 0.2 wt % Nb_2O_5 doped $(Bi_{0.5}Na_{0.5})_{0.94}Ba_{0.06}TiO_3$ (BNBT6N0.2) -PVDF 0-3 composites with 10, 20, and 30 vol. percentage of BNBT6N0.2 at different frequencies between1kHz- 1MHz. Analysis of X-ray diffraction data confirmed the formation of tetragonal unit cell structure for calcined BNBT6N0.2 ceramic. SEM micrographs for 0-3 composites showed dense homogeneous distribution of almost spherical grains in all the composite samples. Conduction mechanism in the material system is explained on the basis of Jump Relaxation hopping model of charge carriers. The complex impedance, electric modulus and electrical conductivity data as the functions of temperature and frequency indicated the presence of grain-boundary effect along with the bulk contribution, especially at higher temperatures and negative temperature coefficient of resistance (NTCR) behaviour of the test ceramic-polymer composites. Ceramic filler concentration dependent increase of d_{33} of the composite is seen to follow the first order exponential growth type of equation.

References

[1]. C. Cui, R.H. Baughman, Z. Igbal, T.R. Kazmar, D.K. Dalstrom, Improved piezoelectric ceramic/polymer composites for hydrophone applications, Synthetic Mat. 85, 1997, 1391-1392.

[2]. C.J. Das, D.K. Das-Gupta, Inorganic ceramic/polymer ferroelectric composite electrets, IEEE Transactions on Dielectrics and Electrical Insulation 3 , 1996, 706-734.

[3]. N.S. Shenck, J.A. Paradiso, Energy scavenging with shoe-mounted piezoelectrics, IEEE Micro. 21, 2001, 30–42.

[4]. J. Granstorm, J. Feenstra, H.A. Sodano, K. Farinholt, Energy harvesting from a backpack instrumented with piezoelectric shoulder straps, Smart Mater. Struct. 16, 2007, 1810–1820.

[5]. L. Wu, L. Chen, C. Liu, Acoustic energy harvesting using resonant cavity of a sonic crystal, Appl. Phys. Lett. 95, 2009, 013506.

[6]. D. Wang, H. Ko, Piezoelectric energy harvesting from flow-induced vibration, J. Micromech. Microeng. 20, 2010, 025019.

[7]. W.SUN, B.LIU, CHARACTERISATION OF PROTON-IRRADIATED 65PMN–35PT/P (VDF–TRFE) 0–3 COMPOSITES MATER. SCI. ENGG. B 127, 2006, 144-149.

[8]. Z. Kutnjak, B. Vodopivec, D. KuöËer, M. Kosec, V. Bobnar, and B. Hilczer, Calorimetric and dielectric study of vinylidene fluoride-trifluoroethylene-based composite, J. Non-Cryst. Solids, 351, 2005, 1261-1265.

[9]. S.H. Xie, B.K. Zhu, X.Z. Wei, Z.K. Xu, and Y.Y. Xu, Polyimide/$BaTiO_3$ composites with controllable dielectric properties, Compos. Part A - Applied Science 36, 2005, 1152-1157.

[10]. Jeong-Hyeon Seol, Jae Shin Lee, Han-Na Ji, Yun-Po Ok, Gyoung Pyo Kong, Ki-Soo Kim, Chang Yoon Kim, Weon-Pil Tai, Piezoelectric and dielectric properties of $(K_{0.44}Na_{0.52}Li_{0.04})$ $(Nb_{0.86}Ta_{0.10}Sb_{0.04})O_3$–PVDF composites, Ceramics International, 38, 2012, S263-S266.

[11]. T. Furukawa, K. Fujino, and E. Fukada, Electromechanical properties in the composites of epoxy resin and PZT ceramics, Japanese Journal of Applied Physics, 15, 1976, 2119–2129.

[12]. W.W. Clegg, D.F.L. Jenkins, and M.J. Cunningham, The preparation of piezoceramic–polymer thick films and their application as micromechanical actuators. Sensors and Actuators A, 58, 1997, 173–177.

[13]. W.K. Sakamoto, S. Shibatta-Kegesawa, D.H.F. Kanada, and D.K. Das-Gupta, Electrical properties of a composite of polyurethane and ferroelectric ceramics. Journal of Materials Science, 33, 1998, 3325–3329.

[14]. H.C. Pant, M.K. Patra, A. Verma, S.R. Vadera, and N. Kumar, Study of the dielectric properties of Barium Titanate–polymer composites. Acta Materialia, 54, 2006, 3163–3169.

[15]. L.A. Ramajo, M.M. Reboredo, and M.S. Castro, Characterisation of epoxy/$BaTiO_3$ composites processed by dipping for integral capacitor films (ICF). Journal of Materials Science, 42, 2007, 3685–3691.

[16]. X.X. Wang, K.H. Lam, X.G. Tang, H.L.W. Chan, Dielectric characteristics and polarization response of lead-free ferroelectric $(Bi_{0.5}Na_{0.5})_{0.94}Ba_{0.06}TiO_3$-P(VDF-TrFE) 0-3 composites, Solid State Communications, 130, 2004, 695-699.

[17]. K.H. Lam, X. Wang, H.L.W. Chan, Piezoelectric and pyroelectric properties of $Bi_{0.5}Na_{0.5})_{0.94}Ba_{0.06}TiO_3$/P (VDF-TrFE) 0-3 composites, Composites. Part A - Appl. Physics, 36, 2005, 1595-1599.

[18]. K. Prasad, A. Prasad, K.P. Chandra, A.R. Kulkarni, Electrical Conduction in 0-3 $BaTiO_3$/PVDF Composites, Integrated Ferroelectrics, 117, 2010, 55-67.

[19]. T. Takenaka., A. Huzumi, T. Hata, and K. Sakata, Mechanical properties of $(Bi, Na)_{1/2}TiO_3$-based piezoelectric ceramics. Silicates Industrials 7(8), 1993. 136-142.

[20]. X.X. WANG, H.L.W. CHAN, C.L. CHOY, PIEZOELECTRIC AND DIELECTRIC PROPERTIES OF CeO_2-ADDED $(BI_{0.5}NA_{0.5})_{0.94}BA_{0.06}TIO_3$ LEAD-FREE CERAMICS, SOLID STATE COMMUN. 125, 2003, 395–399.

[21]. S.J. WU, Q. XU, X.Z. ZHAO, T. LIU, Y.M. LI, PROCESSING AND PROPERTIES OF CeO_2-DOPED FERROELECTRIC $(NA_{0.5}BI_{0.5})_{0.94}BA_{0.06}TIO_3$, MATER. LETT. 60, 2006, 1453–1458.

[22]. H. D. Li, C. D. Feng, and P. H. Xiang, Electrical properties of La^{3+} doped $Na_{0.5}Bi_{0.5})_{0.94}Ba_{0.06}TiO_3$ ceramics. Jpn. J. Appl. Phys., 42, 2003, 7387–7391.

[23]. A. K. Roy, A. Singh, K. Kumari, K. Amaranth, A. Prasad, K. Prasad, Electrical properties and ac conductivity of $(Bi_{0.5}Na_{0.5})_{0.94}Ba_{0.06}TiO_3$ ceramic, ISRN Ceramics, vol. 2012, 2012, Article ID 854831, 10 pages. http://dx.doi.org/10.5402/2012/854831.
[24]. Hongqiang Wang, Ruzhong Zuo, Yi Liu, Jian Fu, "Densification behavior, microstructure, and electrical properties of sol–gel-derived niobium-doped $(Bi_{0.5}Na_{0.5})_{0.94}Ba_{0.06}TiO_3$ ceramics" J. Mater. Sci. 45, 2010, 3677-3682.
[25]. B.J. Chu, D.R. Chen, G.R. Li, Q.R. Yin, "Electrical properties of $Na_{1/2}Bi_{1/2}TiO_3$-$BaTiO_3$ ceramics", J. Eur. Ceram. Soc. 22, 2002, 2115–2121.
[26]. A. Herabut, A. Safari, Processing and electromechanical properties of $(Bi_{1/2}Na_{1/2})_{(1-1.5x)}La_xTiO_3$, J. Am. Ceram. Soc., 80, 1997, 2954–2958.
[27]. J. Yoo, J. Hong, H. Lee, Y. Jeong, B. Lee, H. Song, J. Kwon, Piezoelectric and dielectric properties of La_2O_3 added Bi (Na,K)TiO_3–$SrTiO_3$ ceramics for pressure sensor application Sensors Actu. A 126, 2006, 41–47.
[28]. K. PENGPAT, S. HANPHIMOL, S. EITSSAYEAM, U. INTATHA, G. RUJIJANAGUL, T. TUNKASIRI, MORPHOTROPIC PHASE BOUNDARY AND ELECTRICAL PROPERTIES OF LEAD-FREE BISMUTH SODIUM LANTHANUM TITANATE—BARIUM TITANATE CERAMICS J ELECTROCERAM. 16, 2006, 301–305.
[29]. K. Sambasiva Rao, K. Varada Rajuluua, B. Tilak, A Swathi, Effect of Ba^{2+} in BNT ceramics on dielectric and conductivity properties, Natural Science 2, 2010, 357-367.
[30]. M. J. Forbess, S. Seraji, Y. Wu, C. P. Nguyen, G. Z. Cao, Dielectric properties of layered perovskite $Sr_{1-x}A_xBi_2Nb_2O_9$ ferroelectrics (A = La, Ca and x = 0, 0.1), Applied Physics Letters, 76, 2000, 2934–2936.
[31]. K. Funke, Jump relaxation in solid electrolytes, Progress in Solid State Chemistry, 22(2), 1993, 111–195.
[32]. S. R. Elliot, AC conduction in amorphous chalcogenide and pnictide semiconductors, Advances in Physics, 36, 1987, 135–217.
[33]. F. A.Kröger and H. J. Vink, Relations between the concentrations of imperfections in crystalline solids, Solid State Phys, 3, 1956, 307-435.
[34]. S. Sumi, P. Prabhakar Rao, M. Deepa, and Koshy Peter, Electrical conductivity and impedance spectroscopy studies of cerium based aeschynite type semiconducting oxides $CeTiMO_6$ (M = Nb or Ta), J. Appl. Phys. 108, 2010,063718.
[35]. Pelaiz-Barranco A, Gutierrez-Amador MP, Huanosta A and Valenzuela R Appl Phys Lett 73, 1998, Article ID 2039, 3 pages.
[36]. A. A. Youssef Ahmed, "The permittivity and AC conductivity of the layered perovskite [(CH3)(C6H5)3P]3HgI4," Z. Naturforsch, vol. 57, 2002, 263–269.

Table 1. AC Conductivity based activation energy for 0.2wt% Nb_2O_5 doped $(Bi_{0.5}Na_{0.5})_{0.94}Ba_{0.06}TiO_3$ (BNBT6N0.2)-PVDF 0-3 composites having 10, 20 and 30 volume percentage of BNBT6N0.2 at different indicated frequencies in the high temperature region 115^{o}C -145^{o}C

Volume fraction of ceramic	Activation Energy (eV)	
	at 1kHz	at 10kHz
10	0.596	0.644
20	0.135	0.080
30	0.223	0.196

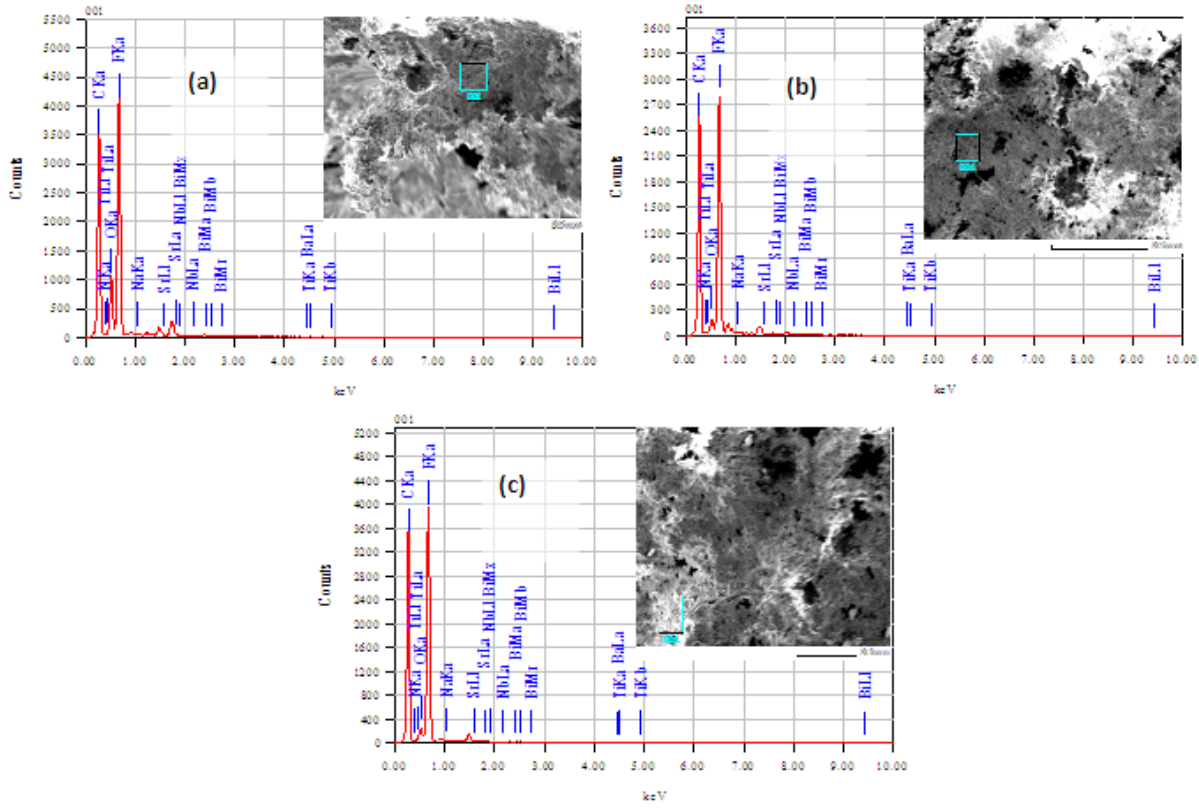

Fig.1. EDAX patterns and SEM micrographs (insets) of 0.2 wt% Nb_2O_5 doped $(Bi_{0.5}Na_{0.5})_{0.94}Ba_{0.06}TiO_3$ (BNBT6N0.2)-PVDF 0-3 composites having (a) 10, (b) 20 and (c) 30 vol.% of BNBT6N0.2

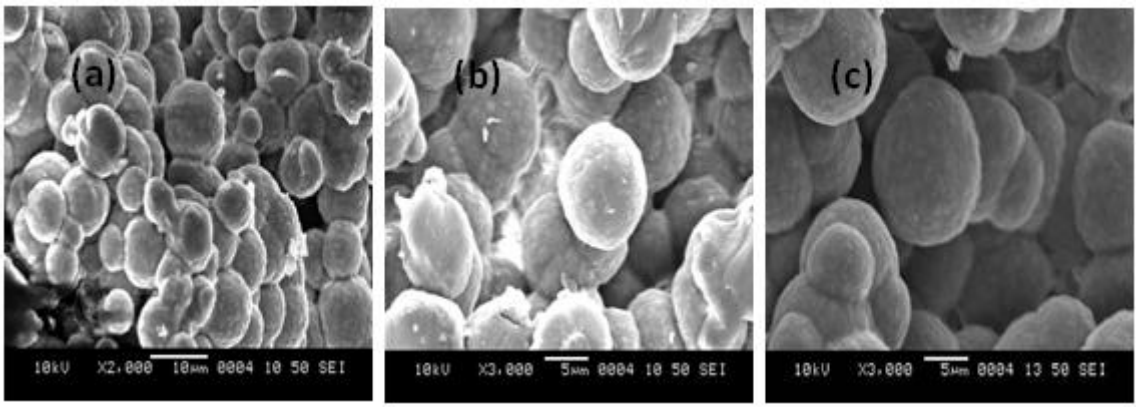

Fig. 2. SEM micrographs of 0.2wt.% Nb_2O_5 doped $(Bi_{0.5}Na_{0.5})_{0.94}Ba_{0.06}TiO_3$ (BNBT6N0.2)-PVDF 0-3 composites having (a) 10, (b) 20 and (c) 30 vol.% of BNBT6N0.2

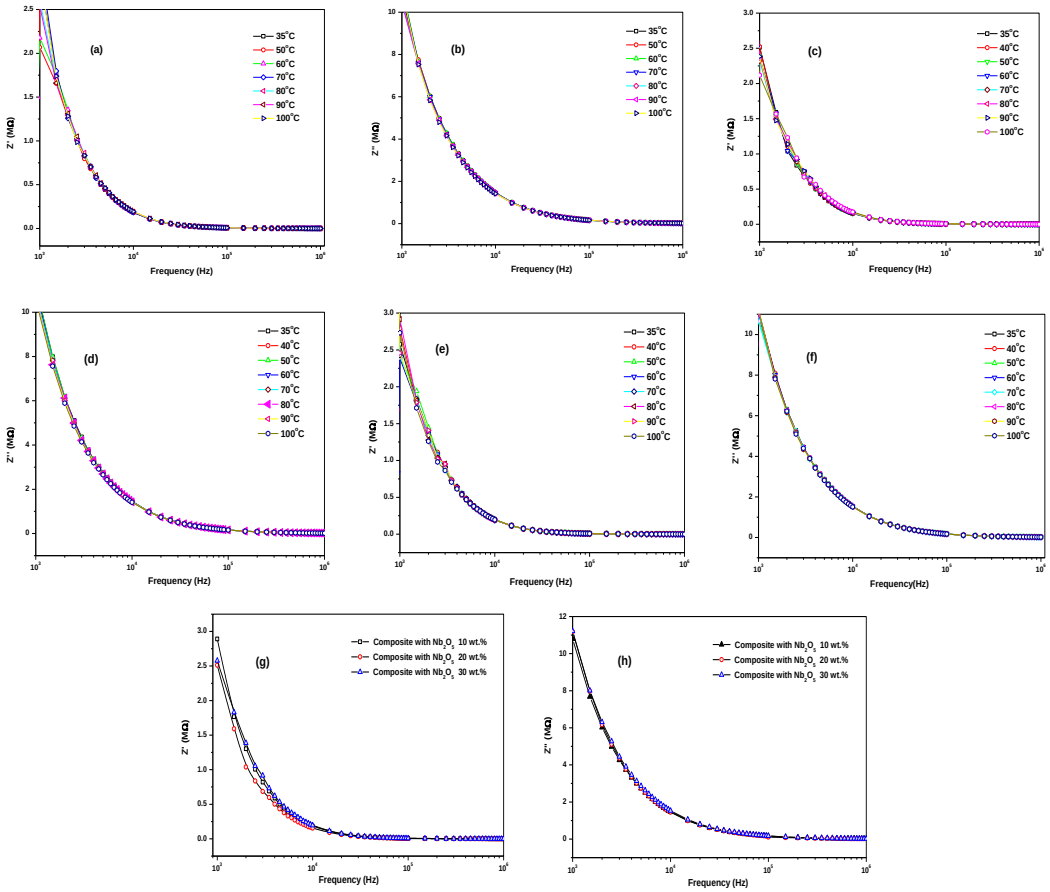

Fig.3(a)-(f): Frequency dependence of real and imaginary parts (Z' and Z'') of complex impedance of 0.2wt.% Nb_2O_5 doped $(Bi_{0.5}Na_{0.5})_{0.94}Ba_{0.06}TiO_3$ (BNBT6N0.2)-PVDF 0-3 composites having (a) 10, (b) 20 and (c) 30 vol. percentage of NBT6N0.2 at different indicated temperatures. Fig.3 (g)-(h) shows the frequency dependence of real and imaginary parts (Z' and Z''), respectively, for the three compositions at the room temperature

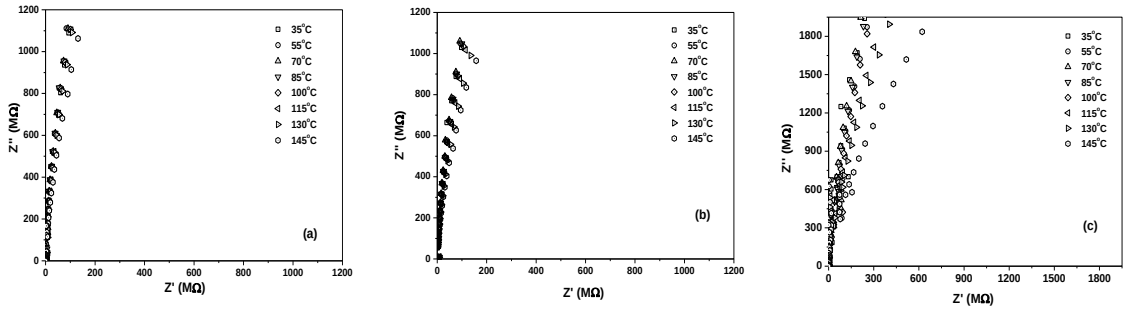

Fig. 4(a)-(c): Nyquist plots for of 0.2wt.% Nb_2O_5 doped $(Bi_{0.5}Na_{0.5})_{0.94}Ba_{0.06}TiO_3$ (BNBT6N0.2)-PVDF 0-3 composites having (a) 10, (b) 20 and (c) 30 vol. percentage of NBT6N0.2 at different indicated temperatures

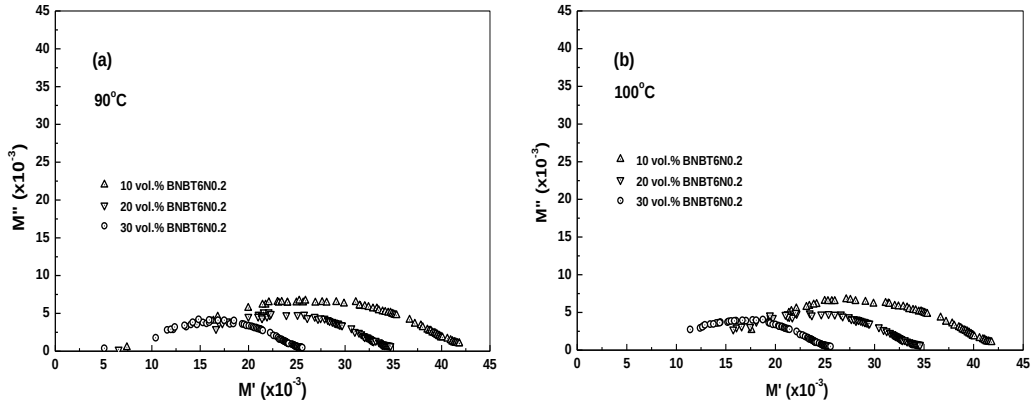

Fig. 5(a) & (b) : Complex modulus plots corresponding to 90°C and 100°C, respectively, for 0.2 wt% Nb_2O_5 doped $(Bi_{0.5}Na_{0.5})_{0.94}Ba_{0.06}TiO_3$ (BNBT6N0.2)-PVDF 0-3 composites with 10, 20 and 30 vol. percentages of BNBT6N0.2

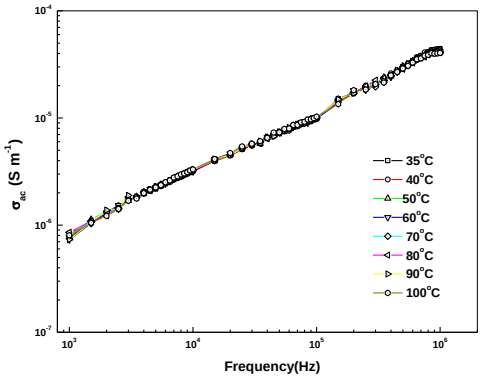

Fig. 6. Frequency dependence of real part of AC conductivity for 0.2 wt. % Nb_2O_5 doped $(Bi_{0.5}Na_{0.5})_{0.94}Ba_{0.06}TiO_3$ (BNBT6N0.2)-PVDF 0-3 composites with 30 vol. percentage of BNBT6N0.2 at different indicated temperatures

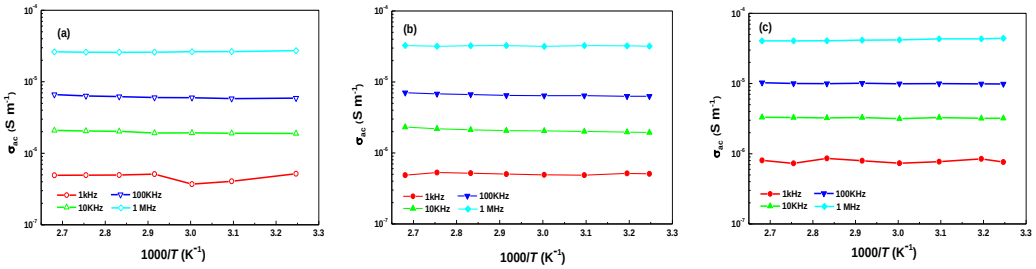

Fig. 7 (a)-(c): Variation of log of the real part of ac conductivity with inverse absolute temperature for 0.2 wt. % Nb_2O_5 doped $(Bi_{0.5}Na_{0.5})_{0.94}Ba_{0.06}TiO_3$ (BNBT6N0.2)-PVDF 0-3 composites with 10, 20, and 30 vol. percentage of BNBT6N0.2 at different indicated frequencies (1kHz, 10kHz, 100kHz, and 1MHz)

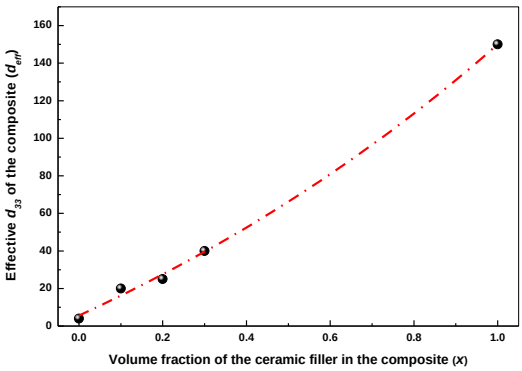

Fig. 8. Ceramic filler concentration dependent piezoelectric coefficient (d_{33}) of $(Bi_{0.5}Na_{0.5})_{0.94}Ba_{0.06}TiO_3$ (BNBT6N0.2)-PVDF 0-3 composites